Stable Polyradicals with High-Spin Ground States. 2. Synthesis and Characterization of a Complete Series of Polyradicals Derived from 2,4,6-Trichloro-$\alpha,\alpha,\alpha',\alpha',\alpha'',\alpha''$-hexakis(pentachlorophenyl)mesitylene with $S = {}^1/_2$, 1, and ${}^3/_2$ Ground States[1,2]

Jaume Veciana,[*,†] **Concepció Rovira,**[†] **Nora Ventosa,**[†] **María Isabel Crespo,**[†] **and Fernando Palacio**[‡]

Contribution from the Institut de Ciència de Materials de Barcelona (CSIC), Campus U.A.B, 08193 Bellaterra, Spain, and Instituto de Ciencia de Materiales de Aragón (CSIC), Universidad de Zaragoza, 50009 Zaragoza, Spain.

Received December 4, 1991. Revised Manuscript Received September 22, 1992

Abstract: The series of stable polyradicals **2–4** was synthesized via the title mesitylene hydrocarbon. Cyclic voltammetry of radicals **2–4** revealed, in accordance with the number of radical centers and their topologies, several reversible one-electron reduction processes. Reduction potentials of the radicals clearly show the existence of mutual electronic interactions between their redox centers. ESR spectra obtained in glassy toluene at low temperature were consistent with **2**, **3**, and **4** in doublet, triplet, and quartet states, respectively. The high-spin states of radicals **3** and **4** were shown to be the ground states by magnetic (susceptibility, magnetization, and ESR) measurements. In addition, such measurements showed that their nearby low–spin states are thermally unaccessible. Polyradicals **3** and **4** exist in several interconvertible stereoisomeric forms. Zero field splitting (zfs) parameters and anisotropic *g* components of such stereoisomeric forms are given. On the basis of the relative values of these magnetic parameters, structural assignations to each one of these stereoisomers have been made. In the case of triradical **4**, its stereoisomeric forms have C_2 and D_3 symmetries and are isolable (HPLC) as solids showing outstanding stabilities (stable in air up to 250 °C).

One of the general approaches to ferro- or superparamagnetism in purely organic molecules is based on large π-conjugated polyradicals with topologically polarized π-spins.[3] Recent synthetic efforts toward this new class of organic materials have resulted in several examples of high-spin organic molecules;[1,4-7] $S = 5$ is the highest spin multiplicity in organic molecules known to date.[4b,5c] The high-spin ground states of these molecules arise, by Hund's rule, from half-filled, multifold, near-degenerate, nonbonding, and nondisjoint HOMOs. Most of these molecules, however, lack sufficient stability for practical purposes,[4,5,7] and in those cases where such instabilities have been overcome, the resulting excited low-spin states are thermally accessible.[6] Until now, such inherent drawbacks have hampered the preparation of large macromolecules possessing both high stabilities and large magnetic moments at room temperature. We, therefore, focused our attention on persistent high-spin molecules having high chemical and thermal stabilities as well as thermally inaccessible excited low-spin states. As has been extensively demonstrated with the unique properties of trivalent carbon radicals of the perchloro triphenylmethyl (PTM) series, chemical and thermal stabilities of free radicals can be increased to exceptional limits by the steric shield produced by bulky chlorine substituents.[8] Using this approach, some examples of highly stable polyradicals having degenerate or close low- and high-spin states have been described.[9] Recently, we have reported two such perchlorinated polyradicals, the *dl* and meso forms of biradical **1**, in which both the highest multiplicity in their ground states and relatively high stabilities were achieved.[1,2] We report here the synthesis and some structural, electrochemical, and magnetic properties of a new complete series of sterically protected polyradicals, **2–4**, with topologically polarized π-spins. Although polyradicals **3** and **4** are not topologically novel as they are derivatives of Schlenk's and Leo's hydrocarbons,[10,11] the simultaneous presence of three large $(C_6Cl_5)_2CH$ or $(C_6Cl_5)_2C^{\bullet}$ subunits increases their thermostabilities to an unprecedented limit not attained in **1**. This fact has permitted the study of these hydrocarbons, achieving novel insights about the mutual influence of several radical centers in a molecule. Worthy of remark is triradical **4**. It exists in two highly symmetric stereoisomeric forms (D_3 and C_2 symmetries) which have quartet ground states and

Chart I

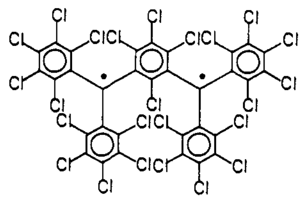

1

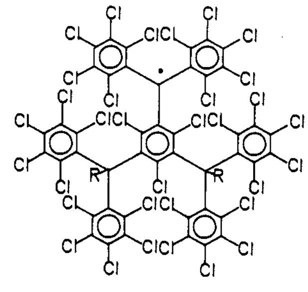

2, R = H, H

3, R = H,•

4, R = •,•

Scheme I[a]

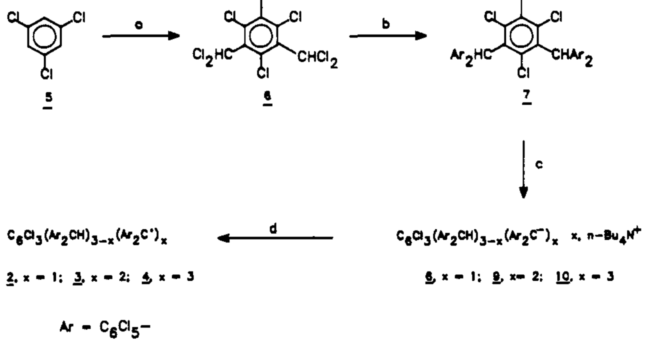

[a] (a) Excess $CHCl_3$, $AlCl_3$, 120 °C, 4 h. (b) Excess C_6HCl_5, $AlCl_3$, 140 °C, 18 h. (c) **8**: 1 equiv of aqueous *n*-$Bu_4N^+OH^-$, THF, 3 h. **9** and **10**: excess aqueous *n*-$Bu_4N^+OH^-$, THF, 5 and 35 days, respectively. (d) Excess *p*-chloranil.

[†] Institut de Ciència de Materials de Barcelona.

[‡] Instituto de Ciencia de Materiales de Aragón.

0002-7863/93/1515-57$04.00/0

thermally unaccessible doublet excited states. The stereoisomeric forms are isolable as stable solids that have outstanding stabilities since they do not show any sign of decomposition up to 250 °C, even in air.

Results and Discussion

The synthesis of radicals **2**–**4** is outlined in Scheme I. 1,3,5-Trichlorobenzene (**5**) was converted to the hexaphenyl-substituted mesitylene **7** via two successive Friedel–Crafts alkylations. Treatment of hydrocarbon **7** in tetrahydrofuran (THF) with tetrabutylammonium hydroxide (aqueous $n\text{-}Bu_4N^+OH^-$) gave carbanions **8**, **9**, and **10** to different extents, depending on the excess of base and reaction times used. Nevertheless, the generation in solution of each one of these carbanions can be controlled by the modification of both reaction conditions. Thus, the treatment of **7** with 1.1 equiv of $n\text{-}Bu_4N^+OH^-$ gave monocarbanion **8**, while polycarbanions **9** and **10** were generated with a large excess (30–40 equiv) of this base using different reactions times—5 days for **9** and 35 days for **10**. The selective generation of dicarbanion **9** from **7**, even when a large excess of the base is used, is explained by the large difference between the rate constants for the individual deprotonation steps **8** → **9** and **9** → **10**. The extremely slow rate observed in the generation of tricarbanion **10** from **9** is ascribed to strong Coulombic repulsions involved in this acid–base reaction. Finally, solutions of carbanions **8**–**10** were oxidized with *p*-chloranil, giving radicals **2**–**4**, respectively.

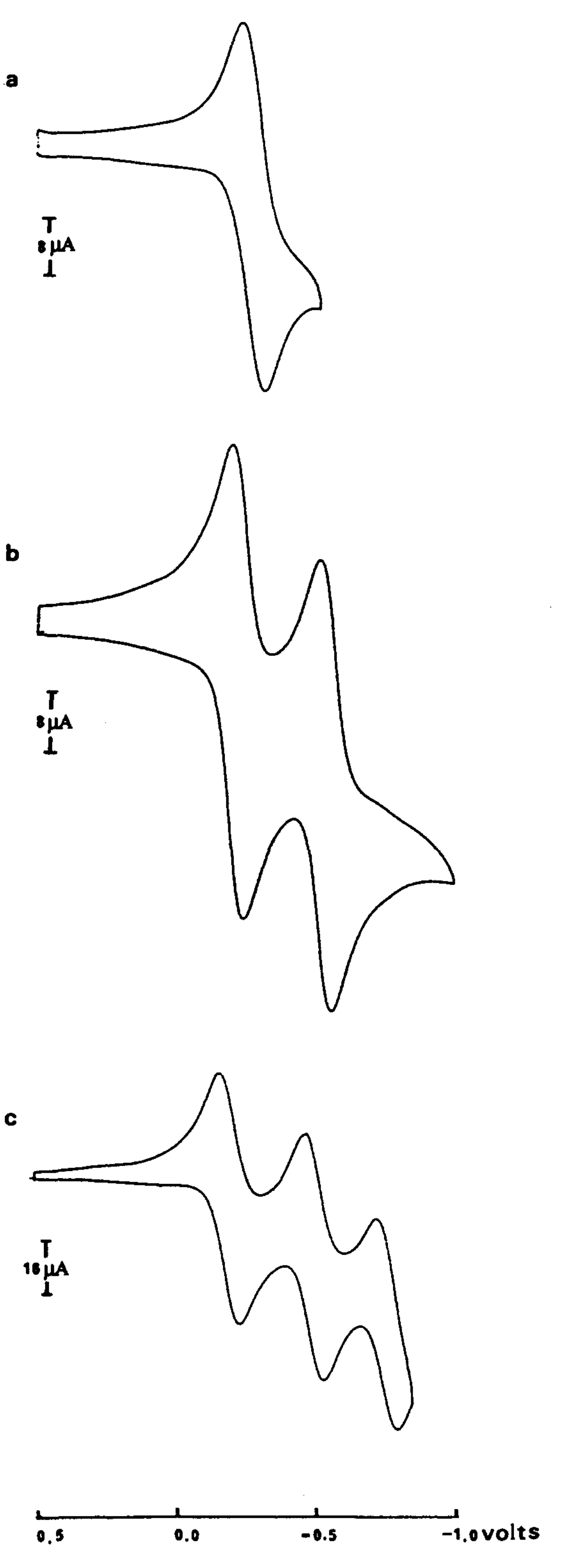

Figure 1. Cyclic voltammograms of radicals **2**–**4** in CH_2Cl_2 (3×10^{-4} M) solution (0.1 M $Bu_4N^+PF_6^-$ as electrolyte, Pt button (working), Pt wire (auxiliary), and SCE (reference) electrodes): (a) monoradical **2**; (b) diradical **3**; (c) triradical **4**.

Due to the low specificity of the acid–base reaction used for the generation of carbanions **8**–**10**, each one of their radical derivatives, **2**–**4**, was slightly contaminated with other members of the polyradical series, as ascertained by HPLC chromatography

---

(1) Part I: Veciana, J.; Rovira, C.; Crespo, M. I.; Armet, O.; Domingo, V. M.; Palacio, F. *J. Am. Chem. Soc.* **1991**, *113*, 2552.

(2) Part of this work was presented at the NATO Advanced Research Workshop on Molecular Materials, Il Giocco, Lucca, Italy, October 28–November 2, 1990. Veciana, J.; Rovira, C. Stable Polyradicals with High Spin Ground States. In *Magnetic Molecular Materials*; Gatteschi, D., Kahn, O., Miller, J., Palacio, F., Eds.; Kluwer Academic Publishers: Dordrecht, The Netherlands, 1991; p 121.

(3) Mataga, N. *Theor. Chim. Acta* **1968**, *10*, 372. Tyutyulkov, N.; Polansky, O. E.; Schüster, P.; Karabunarliev, S.; Ivanov, C. I. *Theor. Chim. Acta* **1985**, *67*, 211.

(4) (a) Murata, S.; Iwamura, H. *J. Am. Chem. Soc.* **1991**, *113*, 5547. (b) Fujita, I.; Teki, Y.; Takui, T.; Kinoshita, T.; Itoh, K.; Miko, F.; Sawaki, Y.; Izuoka, A.; Sugawara, T.; Iwamura, H. *J. Am. Chem. Soc.* **1990**, *112*, 4074. (c) Sugawara, T.; Bandow, S.; Kimura, K.; Iwamura, H.; Itoh, K. *J. Am. Chem. Soc.* **1986**, *108*, 368. (d) Sugawara, T.; Bandow, S.; Kimura, K.; Iwamura, H.; Itoh, K. *J. Am. Chem. Soc.* **1984**, *106*, 6449. (e) Takui, T.; Itoh, K. *Chem. Phys. Lett.* **1973**, *19*, 120. (f) Itoh, K. *Chem. Phys. Lett.* **1967**, *1*, 235. (g) Wasserman, E.; Murray, R. W.; Yager, W. A.; Trozzolo, A. M.; Smolinsky, G. *J. Am. Chem. Soc.* **1967**, *89*, 5076. (h) Brosser, W.; Kurrek, H.; Niemeier, W.; Plato, M. *Tetrahedron* **1975**, *31*, 1769. (i) Snyder, G. J.; Dougherty, D. A. *J. Am. Chem. Soc.* **1985**, *107*, 1774; **1986**, *108*, 299; **1989**, *111*, 3927. (j) Novak, J. A.; Jain, R.; Dougherty, D. A. *J. Am. Chem. Soc.* **1989**, *111*, 7618. (k) Berson, J. A. *Acc. Chem. Res.* **1978**, *11*, 446. Seeger, D. E.; Berson, J. A. *J. Am. Chem. Soc.* **1983**, *105*, 5144 and 5146. (l) Dowd, P. *J. Am. Chem. Soc.* **1970**, *92*, 1066. Dowd, P. *Acc. Chem. Res.* **1972**, *5*, 242. Dowd, P.; Chang, W.; Paik, Y. H. *J. Am. Chem. Soc.* **1986**, *108*, 7416; **1987**, *109*, 5284. (m) Roth, W. R.; Langer, R.; Bartmann, M.; Stevermann, B.; Maier, G.; Reisenaner, H. P.; Sustmann, R.; Müller, W. *Angew. Chem., Int. Ed. Engl.* **1987**, *26*, 256. Haider, K.; Platz, M. S.; Despres, A.; Lejeune, V.; Migirdieyan, E.; Bally, T.; Haselback, E. *J. Am. Chem. Soc.* **1988**, *110*, 2318.

(5) (a) Rajca, A. *J. Am. Chem. Soc.* **1990**, *112*, 5890. (b) Rajca, A.; Utamapanya, S.; Xu, J. *J. Am. Chem. Soc.* **1991**, *113*, 9235. (c) Rajca, A.; Utamapanya, S.; Thayumanavan, S. *J. Am. Chem. Soc.* **1992**, *114*, 1884.

(6) Ishida, T.; Iwamura, H. *J. Am. Chem. Soc.* **1991**, *113*, 4238.

(7) For recent examples of this type of molecules, see: Iwamura, H. *Adv. Phys. Org. Chem.* **1990**, *26*, 179. Gatteschi, D., Kahn, O., Miller, J., Palacio, F., Eds. *Magnetic Molecular Materials*; Kluwer Academic Publishers: Dordrecht, The Netherlands, 1991; and references cited therein.

(8) Ballester, M. *Acc. Chem. Res.* **1985**, 380. Armet, O.; Veciana, J.; Rovira, C.; Riera, J.; Castañer, J.; Molins, E.; Rius, J.; Miravitlles, C.; Olivella, S.; Brichfeus, J. *J. Phys. Chem.* **1987**, *91*, 5608. Ballester, M. *Adv. Phys. Org. Chem.* **1989**, *25*, 267 and references therein. Ballester, M.; Pascual, I.; Torres, J. *J. Org. Chem.* **1990**, *55*, 3035. Ballester, M.; Pascual, I.; Riera, J.; Castañer, J. *J. Org. Chem.* **1991**, *56*, 217. Ballester, M.; Pascual, I. *J. Org. Chem.* **1991**, *56*, 4314.

(9) Ballester, M.; Riera, J.; Castañer, J.; Badía, C.; Monsó, J. M. *J. Am. Chem. Soc.* **1971**, *93*, 2215. Ballester, M.; Riera, J.; Castañer, J.; Ibañez, A. *Tetrahedron Lett.* **1980**, *21*, 2435. Ballester, M.; Veciana, J.; Riera, J.; Castañer, J.; Rovira, C.; Armet, O. *J. Org. Chem.* **1986**, *51*, 2472. Rovira, C.; Veciana, J.; Armet, O.; Castañer, J.; Riera, J.; Vincent, E.; Radhakrishna, P. *Mol. Cryst. Liq. Cryst.* **1988**, *156*, 301. Carilla, J.; Juliá, L.; Riera, J.; Brillas, E.; Garrido, J. A.; Labarta, A.; Alcalá, R. *J. Am. Chem. Soc.* **1991**, *113*, 8281.

(10) Schlenk, W.; Brauns, M. *Ber. Dtsch. Chem. Ges.* **1915**, *48*, 661. Kothe, G.; Denkel, K.-H.; Summermann, W. *Angew. Chem., Int. Ed. Engl.* **1970**, *9*, 906. Luckhurst, G. R.; Pedulli, G. F. *J. Chem. Soc. B* **1971**, 329.

(11) Leo, M. *Ber. Dtsch. Chem. Ges.* **1937**, *70*, 1691. Schmauss, G.; Baumgärtel, H.; Zimmermann, H. *Angew. Chem., Int. Ed. Engl.* **1965**, *4*, 596. Wilker, W.; Kothe, G.; Zimmermann, H. *Chem. Ber.* **1975**, *108*, 2124.

and ESR spectroscopy (vide infra). Thus, diradical **3** was present as an impurity in samples of monoradical **2** (~6%) and triradical **4** (<1%), while monoradical **2** was the contaminant (~2%) of diradical **3**. Radicals **2–4** were isolated as stable, deep red crystalline powders. They have remained unchanged in air for more than 1 year and do not show any significant thermal decomposition when heated at 250 °C for 1 h in air. As occurs with most polychloro triphenylmethyl radicals,[8] solutions of **2–4** were completely stable in the dark, showing slow decomposition when they were exposed to UV or visible light. This behavior contrasts with that observed for biradical **1**, which decomposes in solution even in the dark.[1] The higher stabilities of polyradicals **3** and **4** are, therefore, ascribed to the simultaneous presence of three $(C_6Cl_5)_2C^\bullet$ or $(C_6Cl_5)_2CH$ subunits, instead of only two subunits in **1**. This structural characteristic increases the conformational rigidity of **3** and **4** (vide infra), hindering possible structural reorganizations. It is worth mentioning the overwhelming chemical and thermal stabilities of polyradicals **3** and **4**, since most of the organic high-spin molecules reported to date are stable only in dilute media and at very low temperature.[4,5,7] Only a few such species have been obtained as solids which are, however, stable only under mild conditions.[6,12]

Cyclic voltammetry of radicals **2–4** revealed several reversible stepwise one-electron reduction processes.[13] While triradical **4** showed three reversible waves at −0.19, −0.49, and −0.75 V versus SCE for the 0/−1, −1/−2, and −2/−3 redox couples, diradical **3** revealed two waves at −0.22 and −0.54 V for the 0/−1 and −1/−2 couples, and monoradical **2** showed only one wave at −0.27 V for the 0/−1 event (Figure 1). Such radicals also showed partially reversible oxidation waves corresponding to radical cations and polycations which were located in the positive potential range of 1.5–1.9 V. Two trends are especially significant in the CV reduction waves of this series of polyradicals:[14] (i) Successive replacement of Ar_2CH by $Ar_2C^\bullet$ subunits enlarges the number of accessible redox states, increasing the energy gap between the lowest and highest charged states. (ii) The potentials of existing redox states shift to less negative values when the next highest homologue is reduced. Both trends are a clear indication of the mutual interactions between the redox centers existing in these molecules and can be completely explained from qualitative arguments on the basis of only intramolecular electronic effects.[15] Thus, intramolecular Coulombic repulsions would explain the observed increasing destabilization of species with higher negative charges, while cross-conjugation, due to the molecular topology, between negative and radical centers would explain the higher stabilization of partially charged species with a larger number of radical centers. Nevertheless, solvent effects could also play a role in the relative stabilization of negatively charged species.[16] A detailed study of the medium effects on these reduction processes and their contribution to the relative stabilization of involved species, as well as the study of the oxidation processes of electroactive polyradicals **2–4**, is in progress and will be published elsewhere.[17]

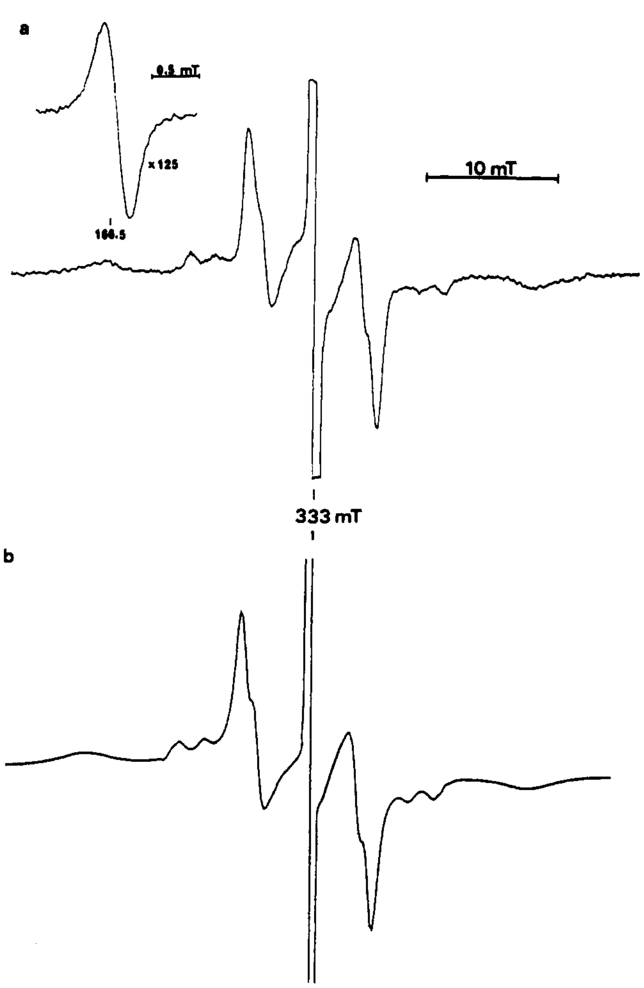

Figure 2. (a) Experimental first derivative ESR spectrum of diradical **3** in frozen toluene at 123 K. Insert shows the observed signal corresponding to the $\Delta M_s = \pm 2$ forbidden transition of stereoisomeric triplets. (b) Simulated spectrum obtained by summation of a doublet impurity (~2% of monoradical **2**) and three randomly oriented triplets with different relative abundances (59%, **3A**; 16%, **3B**; 23%, **3C**), distinct zfs parameters, and g values (see text). Lorentzian line shapes with half-widths at half-height of 1.2, 0.6, 0.6, and 0.1 mT were used for the simulation of triplets **3A**, **3B**, and **3C** and the impurity of monoradical **2**, respectively.

X-band ESR spectra of radicals **2–4** in dilute toluene solutions at room temperature showed symmetrical signals at $g_{iso} = 2.0024$, 2.0026, and 2.0026 with peak to peak line widths of 0.12, 0.36, and 0.40 mT, respectively. The larger line widths observed for polyradicals **3** and **4** indicate that dipole–dipole interactions among the unpaired electrons are moderate, i.e., $|D| \ll h\nu$, in both compounds.[1] Thus, the application of the perturbation theory to the analysis of their ESR fine structures is guaranteed. In frozen toluene matrices, polyradicals **3** and **4** showed strong well-resolved symmetrical features indicative of the presence, in both cases, of several randomly oriented species in high-spin states. In the spectrum of biradical **3** (Figure 2a), a center line was clearly observed, together with these symmetrical features. This center line, $g_{xx} \approx g_{yy} \approx g_{zz} = 2.0024$, corresponds to a doublet impurity of monoradical **2** and, typically, its intensity amounts to 2% of the total spectrum intensity,[18] as ascertained by ESR simulation

---

(12) For examples of organic high-spin molecules with enhanced stabilities, see: Fisher, H. F.; Hellewge, K. H.; Landolt-Börnstein, 11 *Magnetic Properties of the Free Radicals*; Kothe, G., Wilher, J., Eds.; Springer-Verlag: Berlin, 1980; Vol. 9, pp 148–189.

(13) Since the electrode processes are Nernstian, the reduction potentials—in terms of reversible half-wave potentials—were taken as the average of the reduction and oxidation peak potentials for each reduction step.

(14) Such trends are similar to those reported for the reductive charging–discharging behavior of oligomers of the phenylene–vinylene type which have unstable radical centers (see: Heinze, J.; Mortensen, J.; Müllen, K.; Schenk, R. *J. Chem. Soc., Chem. Commun.* **1987**, 701) and contrast with those described for other triphenylmethane derivatives (see: Kothe, G.; Sümmermann, W.; Baumgärtel, H.; Zimmermann, H. *Tetrahedron* **1972**, *28*, 5949 and 5957.

(15) Consecutive CV reduction waves are separated by −320 mV for diradical **3** and by −300 and −260 mV for triradical **4**. Such separations are significantly more than the −35.6 mV difference expected for two one-electron transfers from two noninteracting redox centers at 25 °C. (In multistep one-electron transfers of molecules containing k equivalent, noninteracting, reducible centers, the potential separation between the first and the kth electron transfer should be $-(2RT/F)\ln k$; see: Bard, A. J.; Faulkner, L. R. *Electrochemical Methods*; Wiley: New York, 1980; Chapter 6, p 234.) Therefore, it is clear that for **3** and **4** the difficulty in adding the second electron in two one-electron transfer reactions arises mainly from electronic interactions between redox centers.

(16) For a complete discussion of solvent effects in the relative stabilization of multicharged species produced in electrochemical experiments, see: Lichtemberg, D. L.; Johnston, R. L.; Hinkelmann, K.; Suzuki, T.; Wudl, F. *J. Am. Chem. Soc.* **1990**, *112*, 3302 and references cited therein.

(17) Veciana, J.; Claret, J.; Rovira, C. Manuscript in preparation.

Chart II

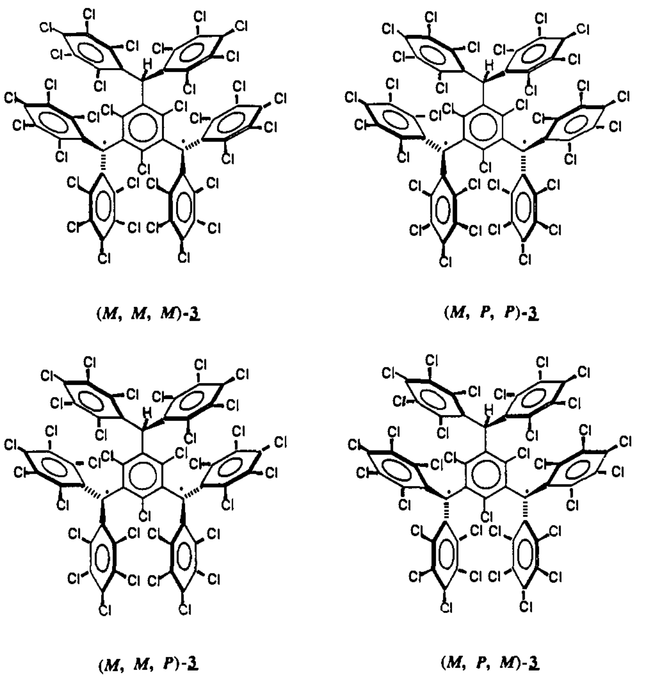
(M, M, M)-3
(M, P, P)-3
(M, M, P)-3
(M, P, M)-3

(Figure 2b).[19] The nature of this impurity, as well as its content, was confirmed later on by analytical HPLC.

The symmetrical features observed in the spectrum of **3** (Figure 2a) were assigned to $\Delta M_s = \pm 1$ transitions of three different triplet species, named **3A**,[20] **3B**, and **3C**. Their relative abundances, zero field splitting (zfs) parameters, and principal *g* components were determined by ESR simulation (Figure 2b)[19] and are as follows: triplet **3A**, 59%, $|D|/hc = 0.0165$ cm^{-1}, $|E|/hc = 0.0047$ cm^{-1}, $g_{xx} \approx 2.0025$, and $g_{yy} = g_{zz} = 2.0010$; triplet **3B**, 16%, $|D|/hc = 0.0074$ cm^{-1}, $|E|/hc \approx 0$ cm^{-1}, $g_{xx} = g_{yy} = 2.0028$, and $g_{zz} = 2.0010$; and triplet **3C**, 23%, $|D|/hc = 0.0092$ cm^{-1}, $|E|/hc \approx 0$ cm^{-1}, $g_{xx} = g_{yy} = 2.0027$, and $g_{zz} = 2.0012$. A broad and intense absorption at the half-field region was also observed in the spectrum of **3** (see insert of Figure 2a). This absorption was ascribed to the forbidden $\Delta M_s = \pm 2$ transitions of the triplet species already mentioned. In order to determine whether these species were ground states or thermally accessible excited states, the temperature dependence of this signal was attempted. It was found that its total intensity follows the Curie law, $I = C/T$ ($r = 0.995$), over the temperature range 123–200 K. This result suggests that the triplet species responsible for this absorption are the ground states, as was confirmed afterward by susceptibility measurements. Compelling evidence for the stereoisomeric nature of the three observed triplet species was provided both by the stereochemical analysis of biradical **3** and by Dynamic-HPLC (D-HPLC) experiments at different temperatures.[21] The stereochemical analysis of **3**, based on previous considerations given by Mislow et al.,[22] predicts four pairs of enantiomers (Chart II),[23,24] for which different abundances and slow isomerizations are expected. This is due to the restricted rotations of pentachlorophenyl groups which are caused by the large steric hindrance produced by bulky ortho chlorine atoms.[26] Stereoisomers of **3** must differ in the helical sense of the three propeller-like $Ar_2C^{\bullet}$ and Ar_2CH subunits, as well as in the relative orientation of the hydrogen atom with respect to the two $Ar_2C^{\bullet}$ subunits.[27]

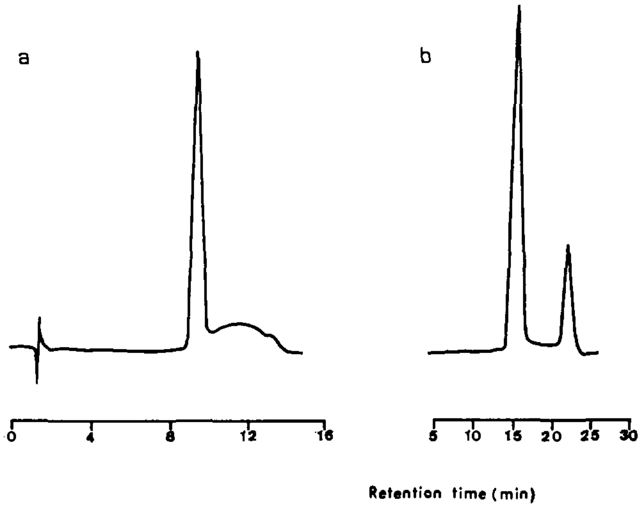

Figure 3. Chromatograms of diradical **3** on an analytical C_{18} reversed-phase column at (a) 300 and (b) 275 K: eluent, CH_3CN/THF (70:30); flow rate, 1 mL min^{-1}; UV detector at 383 nm. Area ratio of the two peaks at 275 K is 77:23.

Because of the different conformations and symmetries of these stereoisomeric triplet species, they must show distinct zfs parameters. The structural assignation of each one of these species was performed by comparing their zfs parameters with those of other triplets with similar conformations, such as the *dl* and meso forms of biradical **1**.[1] Thus, the similarity of the zfs parameters observed for the triplet **3A** and for the meso form of biradical **1** ($|D|/hc = 0.0152$ cm^{-1}, $|E|/hc = 0.0051$ cm^{-1}),[1] as well as the closeness of those corresponding to triplets **3B** and **3C** with those of the *dl*-**1** biradical ($|D|/hc = 0.0085$ cm^{-1}, $|E|/hc < 0.0003$ cm^{-1}),[1] suggests a close resemblance in their spin distributions and structures. On the basis of these similarities, triplet **3A** was tentatively assigned to an enantiomeric pair with its two $Ar_2C^{\bullet}$ subunits arranged as in *meso*-**1**, i.e., with an M^*,P^* relative conformation in the two radical centers: (M,M,P)-**3** + (P,P,M)-**3** and/or (M,P,M)-**3** + (P,M,P)-**3**.[20] Analogously, triplets **3B** and **3C** were assigned to two enantiomeric pairs with their two $Ar_2C^{\bullet}$ subunits as in *dl*-**1**, i.e., with M^*,M^* relative conformations in the two radical centers: (M,M,M)-**3** + (P,P,P)-**3** and (M,P,P)-**3** + (P,M,M)-**3**. On the other hand, D-HPLC experiments, performed in the range 275–300 K, showed distorted chromatographic profiles (Figure 3) seemingly characteristic of an on-column interconversion process between two resolvable compounds.[21] Such behavior is in agreement with theoretical expectations for an $Ar_2CHAr'(C^{\bullet}Ar_2)_2$ system with four pairs of enantiomers and in which the epimerization of the Ar_2CH subunit is much faster than the separation time scale while epimerizations of $Ar_2C^{\bullet}$ subunits are comparable to this time scale.[28] In such a system, an achiral

---

[18] In a randomly oriented glass sample, only a small fraction (species oriented at canonical directions) of a triplet contributes to its signal amplitude. By contrast, in a monoradical with small *g* anisotropy, all of the species contribute equally to its signal amplitude. For this reason, a 2% monoradical impurity in diradical **3** produces the large peak to peak height observed for the central line.

[19] For the simulation of ESR spectra of doublets and triplets, see ref 1 and references cited therein.

[20] The extreme broadness of the outermost experimental lines prevents one from determining whether they are originate from only one or two triplet species. Nevertheless, these lines can be fairly well reproduced by simulation with only one triplet species, named **3A**, with the *g* components and zfs parameters given in the text.

[21] Veciana, J.; Crespo, M. I. *Angew. Chem., Int. Ed. Engl.* **1991**, *30*, 74.

[22] Gust, D.; Mislow, K. *J. Am. Chem. Soc.* **1973**, *95*, 1535. Mislow, K. *Acc. Chem. Res.* **1976**, *9*, 26.

[23] Only four and two diastereoisomeric forms are respectively depicted for diradical **3** (Chart II) and triradical **4** (Chart III). Each one of these forms has its corresponding enantiomer.

[24] Descriptors *P* and *M* denote plus and minus, the rotatory characteristics of a helix, and the asterisks on these descriptors denote relative conformations; see ref 25. In order to give a complete conformational description of each stereoisomer, a convention has been adopted: descriptors of the three helical subunits are ordered starting from that corresponding to a unique subunit (Ar_2CH in **3** and any Ar_2C in **4**) followed by the descriptors corresponding to the subunits arranged clockwise.

[25] Meurer, K. P.; Vögtle, F. *Top. Curr. Chem.* **1985**, *127*, 1–76. Cross, I. C.; Klyne, W. Rules for Nomenclature of Organic Chemistry. IUPAC (Organic Chemistry Division) Commission of Nomenclature of Organic Chemistry. *Pure Appl. Chem.* **1976**, *45*, 11–30.

[26] For related examples, see refs 1 and 21.

[27] Different relative orientations of the H atom can only take place when the propeller helicities of the two Ar_2C subunits are distinct (i.e., when they have an M^*,P^* relative conformation).

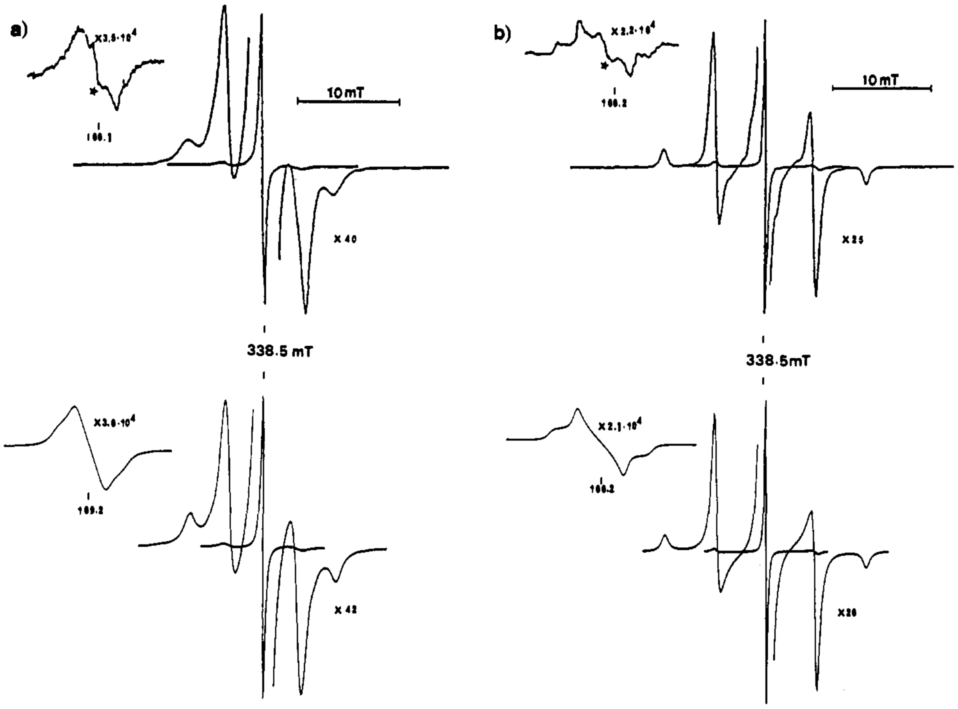

Figure 4. Top: Experimental ESR first derivative spectra at 143 K in glassy toluene of pure samples of (a) C_2-**4** (**4A** quartet) and (b) D_3-**4** (**4B** quartet). Inserts show the observed signals corresponding to $\Delta M_s = \pm 2$ foridden transitions; the asterisks indicate lines corresponding to $\Delta M_s = \pm 2$ forbidden transitions of stereoisomeric forms of triplet **3** present as impurities. Bottom: Simulated spectra for randomly oriented species with (a) $|D|/hc = 0.003\,63$ cm^{-1}, $|E|/hc = 0.000\,09$ cm^{-1}, $g_{xx} = g_{yy} = 2.0029$, $g_{zz} = 2.0012$, and Lorentzian line width (LLW) of 0.80 mT and (b) $|D|/hc = 0.005\,01$ cm^{-1}, $|E|/hc = 0$ cm^{-1}, $g_{xx} = g_{yy} = g_{zz} = 2.0024$, and LLW of 0.42 mT. Inserts show the simulated signals due to $\Delta M_s = \pm 2$ transitions of quartets.

stationary phase (as octadecylsilane) will only be able to recognize the different diastereoisomeric forms arising from the rigid helical conformations of both radical centers since the Ar_2CH subunit is not temporarily rigid. Thus, the two chromatographic peaks observed at 275 K must correspond to triplet species with distinct conformations in the two radical centers (i.e., with M^*,P^* and M^*,M^* relative conformations in such centers). The relative areas of these two peaks (77% and 23%) are close but do not accurately correspond with the relative populations observed in the ESR spectrum for triplet **3A** (60%), with an M^*,P^* conformation, and for the sum of triplets **3B** and **3C** (40%), both with M^*,M^* relative conformations. This result confirms the structural assignations previously given for triplets **3A–C**. The divergence in the stereoisomeric populations observed with these two techniques cannot be considered relevant because both measurements were performed at very different experimental conditions (temperature and solvent media). Indeed, the populations determined from the ESR spectrum correspond to species having the conformations of Ar_2CH subunits frozen out, a situation that must modify the steric energy of the molecules. Therefore, the divergence in the stereoisomeric populations of biradical **3** observed with both techniques is ascribed to the distinct steric strain shown by the isomers when they are in liquid or frozen media.

In the rigid media ESR spectrum of triradical **4**, fine structures corresponding to two quartet species were observed:[29,32] a major quartet (**4A**, 83%) with $|D|/hc = 0.0036$ cm^{-1}, $|E|/hc \approx 0.0001$ cm^{-1}, $g_{xx} \approx g_{yy} = 2.0029$, and $g_{zz} = 2.0012$ and a minor quartet (**4B**, 17%) with $|D|/hc = 0.0050$ cm^{-1}, $|E|/hc = 0$ cm^{-1}, and $g_{xx} = g_{yy} = g_{zz} = 2.0024$. As for diradical **3**, quartets **4A** and **4B** have a diastereoisomeric nature and are also interconvertible in solution. However, the diastereoisomerization energy barrier of **4**,[34] $\Delta G^{\ddagger}_{298K}$ (**4A** → **4B**) = 100 kJ mol^{-1}, is higher than that of **3**[1] permitting, therefore, the isolation of pure samples of **4A** and **4B** quartets by HPLC without any experimental complication. Pure **4A** quartet was also obtained from the diastereoisomeric mixture by re-

Chart III

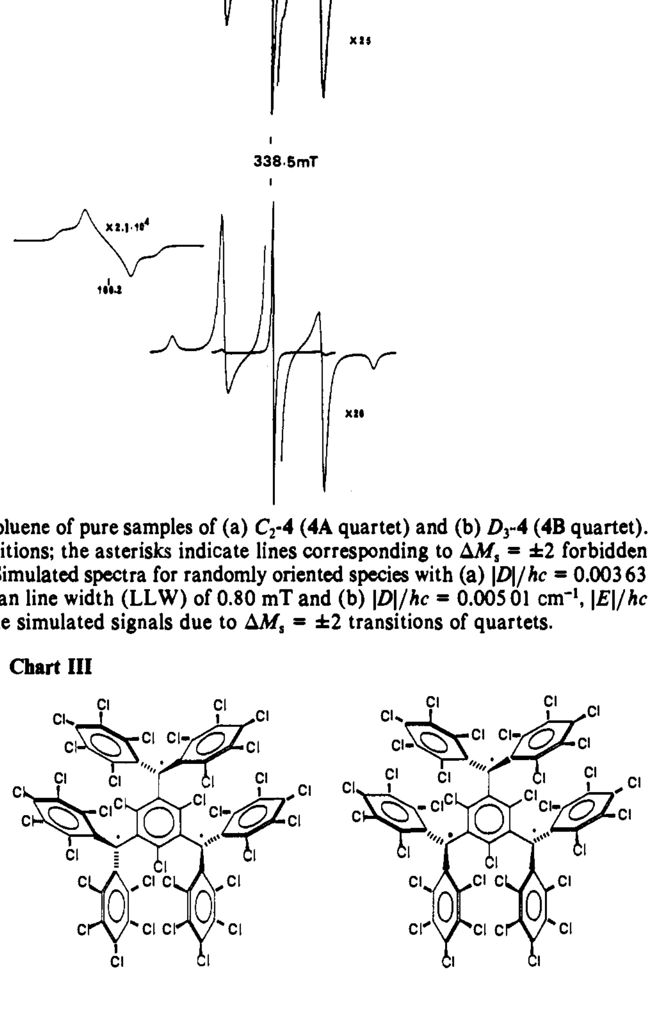

(*M, M, M*)-**4**
D_3 Symmetry

(*M, M, P*)-**4**
C_2 Symmetry

---

(28) Epimerization rates in diradical **3** must be close to the enantiomerization rates of $(C_6Cl_5)_3CH$ and $(C_6Cl_5)_3C^{\bullet}$, since these compounds have similar steric hindrances. At 303 K, the enantiomerization rate of $(C_6Cl_5)_3CH$ is 2 orders of magnitude larger than that of $(C_6Cl_5)_3C^{\bullet}$. Crespo, M. I. Ph.D. Dissertation, Institut Quimic de Sarrià, Barcelona, Spain, 1991.

(29) zfs parameters and principal g components of both quartets were determined by means of the analytical expressions for $|D'|$, $|E'|$, g_{xx}, g_{yy}, and g_{zz} in terms of the H_{zi}, H_{yi}, and H_{xi} magnetic field turning points: $|D'| = (g_{zz}/g_e)(H_{z2} - H_{z1})/4$; $|E'| = (|D'|/3) - (g_{xx}/g_e)(H_{x1} - H_{x2})/6$ (or $|E'| = (g_{yy}/g_e)(H_{y1} - H_{y2})/6 - |D'|/3$); $g_{ii} = h\nu/H$. $H = (H_{z2} + H_{z1})/2$, $H = (H_{y2} + H_{y1})/2$, and $H = (H_{x2} + H_{x1})/2$ were used for calculate g_{zz}, g_{yy}, and g_{xx}, respectively. Such analytical expressions were derived from energy solutions of the spin Hamiltonian, using second-order perturbation theory (see ref 30), and agree with those previously deduced for an $S = {}^3/_2$ system with axial symmetry and an isotropic g factor; see ref 31.

(30) Teki, Y.; Takui, T.; Yagi, H.; Itoh, K.; Iwamura, H. *J. Chem. Phys.* **1985**, *83*, 539. Teki, Y.; Takui, T.; Itoh, K. *J. Chem. Phys.* **1988**, *88*, 6134.

(31) Kothe, G.; Ohmes, E.; Brichmann, J.; Zimmermann, H. *Angew. Chem., Int. Ed. Engl.* **1971**, *10*, 938. Reibish, K.; Kothe, G.; Brickmann, J. *Chem. Phys. Lett.* **1972**, *17*, 86–88. Brickmann, J.; Kothe, G. *J. Chem. Phys.* **1973**, *59*, 2807.

(32) Relative abundances of both quartets were determined either by ESR simulation (see ref 33) of the mixture in frozen toluene at 143 K (**4A**, 83%; **4B**, 17%) or by analytical HPLC separation performed in CH_3CN/THF (70:30) at 298 K (**4A**, 82%; **4B**, 18%).

(33) The simulation of quartet ESR fine structures was carried out with a program written by the authors on the basis of a perturbation treatment to first order in the fine-structure energy, using equations given by Itoh et al.; see ref 30. $|E|/hc$ values greater than 0.0002 cm^{-1} gave simulated spectra with split inner-paired lines.

(34) Detailed thermodynamic and kinetic studies on triradical **4** are underway and will be published elsewhere.

crystallization in benzene. To our knowledge, the isolation as pure compounds of all of the stereoisomers of **4** represents the first example reported for a high-spin molecule.

Figure 4 shows the observed rigid media ESR spectra of pure **4A** and **4B** quartets as well as those spectra obtained by a simulation procedure.[33] As is shown in Figure 4, both the axial resonance fields and the relative peak heights and profiles of the experimental spectra were fairly well reproduced by simulation. Such an agreement is a clear sign of the high purity of **4A** and **4B** and moreover reveals that the high intensities of their center lines is an intrinsic characteristic of quartets. The observed magnitudes of $|E|/hc$ parameters for **4A** (no-null) and **4B** (null) quartets indicate that the last one must have at least a 3-fold symmetry, as is indeed expected from the conformational analysis of triradical **4**. In fact, a molecule with three equidistant propeller-like subunits, each one of its blades having a local 2-fold symmetry, must exist only in two pairs of enantiomers with C_2 and D_3 symmetries (Chart III).[23,24] Therefore, ESR data permit the assignment of the **4A** quartet to the enantiomeric pair with C_2 symmetry, i.e., to (*M,M,P*)-**4** + (*P,P,M*)-**4**, and the **4B** quartet to that with D_3 symmetry, i.e., to (*M,M,M*)-**4** + (*P,P,P*)-**4**. The $|D|/hc$ values observed for C_2-**4** and D_3-**4** quartets are larger to those exhibited by triradicals 4,4′,4″-(benzene-1,3,5-triyl)tris(2,6-di-*tert*-butylphenoxy)[35] (0.0021 cm^{-1}) and 1,3,5-tris[(3,5-di-*tert*-butyl-4-oxo-2,5-cyclohexadien-1-ylidene)(3,5-di-*tert*-butyl-4-oxyphenyl)methyl]benzene[35a,36] (0.0007 cm^{-1}) and are comparable to those reported for 1,3,5-benzenetriyltris(diphenylmethyl) triradical (Leo's hydrocarbon)[11] (0.0049 cm^{-1}) and 1,3,5-benzenetriyltris[bis(biphenyl-4-yl)methyl] triradical,[31] (0.0041 cm^{-1}). Such a result is in accordance with the fact that D values are qualitatively inversely proportional to the size of π-conjugate systems. Furthermore, this result also shows that high distortions and different symmetries of C_2-**4** and D_3-**4**, caused by their bulky ortho chlorine atoms, do not produce significant spin redistributions in their half-filled, 3-fold degenerate, nondisjoint HOMOs. Otherwise their D values would be very different from that of Leo's triradical.

As occurs with most of organic quartets with low D' values,[30] rigid matrix ESR spectra of C_2-**4** and D_3-**4** do not exhibit any resolved off-axis extra lines together with the normal canonical lines associated with $\Delta M_s = \pm 1$ transitions. This is due to the small D' values of C_2-**4** (3.9 mT) and D_3-**4** (5.3 mT), which produce very small angular dependences of the resonance fields leading to overlapping of the off-axis extra lines with the canonical ones.[37]

Besides the canonical lines due to allowed $\Delta M_s = \pm 1$ transitions, rigid matrix ESR spectra of quartets C_2-**4** and D_3-**4** also showed weak absorptions corresponding to forbidden $\Delta M_s = \pm 2$ transitions (Figure 4, top). Overlapped with these absorptions, extremely weak single lines (Figure 4, top; lines labeled with *) were observed. Such lines were tentatively ascribed to forbidden $\Delta M_s = \pm 2$ transitions of the stereoisomers of biradical **3**, present as impurities of C_2-**4** and D_3-**4** quartets. The content of these impurities was estimated to be less than 1% by ESR simulation of these signals. Unfortunately, a direct confirmation by HPLC of the presence of stereoisomers of **3** was not possible because their retention times are very close to those of C_2-**4** and D_3-**4**. Forbidden $\Delta M_s = \pm 2$ transitions of C_2-**4** and D_3-**4** appeared centered at $H_0/2$ with intensities of $\sim {}^1/_{16000}$ and $^1/_{9000}$ of their corresponding $\Delta M_s = \pm 1$ transitions. Both the center positions and the intensities of such absorptions corresponded exactly to theoretical predictions. In addition, singularities of absorption intensities were reproduced reasonably well for both quartets (Figure 4, bottom) by simulation,[33] using the zfs parameters obtained from the allowed transitions. Noteworthy is the ESR fine structure due to forbidden $\Delta M_s = \pm 2$ transitions of the D_3-**4** quartet. The resonance fields, corresponding to singularities of this absorption, appeared well spaced out by 2.7 mT, i.e., by $D'/2$, as theoretically expected.[30,31] To our knowledge, this is the first example of an organic quartet where such a structured ESR line was clearly observed. Finally, no signals assigned to the forbidden $\Delta M_s = \pm 3$ transition were observed for C_2-**4** and D_3-**4** quartets. Such a result is in agreement with the extreme weakness expected for these transitions. Variable-temperature ESR experiments with pure quartets C_2-**4** and D_3-**4** were performed in the temperature range of 130–200 K. Total intensities of their $\Delta M_s = \pm 1$ signals increase linearly with $1/T$ (r = 0.994 and 0.998), indicating that quartets are the ground states of both stereoisomers.

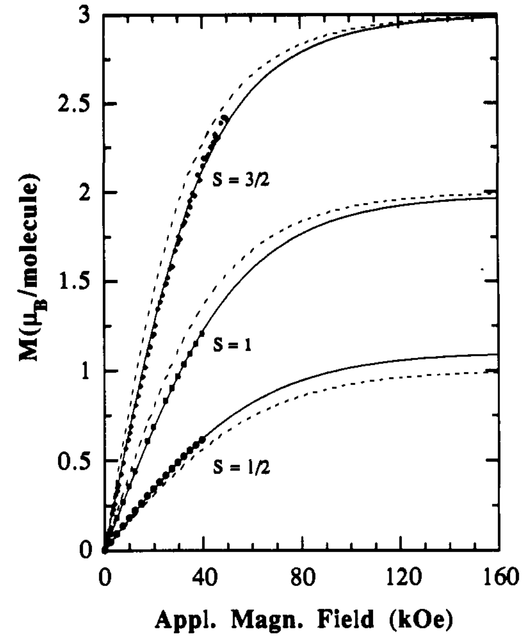

Figure 5. Field strength dependencies of experimental molar magnetizations of radicals **2** (●), **3** (■), and **4** (◆). Solid lines are the calculated molar magnetization curves for $S = {}^1/_2$, 1, and $^3/_2$ species with weak antiferromagnetic intermolecular interactions (see text). Dashed lines are the theoretical molar magnetization curves for $S = {}^1/_2$, 1, and $^3/_2$ ideal paramagnets.

The temperature dependence between 4.2 and 300 K of the magnetic susceptibility of microcrystalline radicals **2**–**4** follows the Curie–Weiss law, with θ = −0.5, −1.1, and −1.1 K and effective magnetic moments 1.79, 2.87, and 3.89 μ_B. These values compare very well with calculated μ_{eff} values for $S = {}^1/_2$, 1, and $^3/_2$ ground states, respectively, and confirm that in this temperature range intramolecular spin alignment for radicals **3** and **4** is complete. No significant difference was observed in the magnetic behavior of pure C_2-**4** or the 82:12 mixture of C_2-**4** and D_3-**4**.

Magnetization measurements of radicals **2**–**4** at 4.2 K in the magnetic field range of 0–5 T are depicted in Figure 5 as a function of the magnetic field H. The data can be compared with the theoretical magnetization curves of an ideal paramagnet for $S = {}^1/_2$, 1, and $^3/_2$, respectively. These curves, represented as dashed lines in Figure 5, are given by

$$M/N\mu_B = gSB_S(x)$$

where N is Avogadro's number, μ_B is the Bohr magneton, g is the gyromagnetic factor, and B_S is the Brillouin function:

$$B_S(x) = \frac{2S+1}{2S}\coth\left(\frac{2S+1}{2S}x\right) - \frac{1}{2S}\coth\left(\frac{1}{2S}x\right)$$

and

$$x = \frac{g\mu_B SH}{kT}$$

---

(35) (a) Gierke, W.; Harrer, W.; Kurreck, H.; Reusch, J. *Tetrahedron Lett.* **1973**, 3681. (b) Novak, C.; Kothe, G.; Zimmermann, H. *Ber. Bunsenges. Phys. Chem.* **1974**, *78*, 265.

(36) Harrer, W.; Kurreck, H.; Reusch, J.; Gierke, W. *Tetrahedron* **1975**, *31*, 1769. Kriste, B.; van Willigen, H.; Kurreck, H.; Möbius, K.; Plato, M.; Biehl, R. *J. Am. Chem. Soc.* **1978**, *100*, 7505.

(37) For quartets with $D' < 120$ mT and axial symmetries, the separations between the two theoretically expected degenerate (see ref 30) off-axis extra lines and the magnetic field turning points, H_{xy0} and H_{z0}, are $35D'^2/18H_0$ and $4D'^2/9H_0$, respectively (expressions derived from the equations of resonance fields are given to the second order in ref 30).

where k is the Boltzmann constant and T the temperature.

It is clear that radicals **3** and **4** are more slowly magnetized than an ideal paramagnet, while apparently radical **2** is magnetized more rapidly. However, as we already have mentioned, monoradical **2** contains a small fraction of biradical **3**, which tends to increase the magnetization of the sample. If the experimental data of **2** are corrected from the impurity content of **3**, then its magnetization also goes below that of an ideal paramagnet. The behavior is indicative of the presence of weak antiferromagnetic interactions in the compounds, in full agreement with the susceptibility results.

Magnetization experiments are important because they provide a direct and independent determination of the spin values of the radical samples. Comparison of experimental data with magnetization of pure paramagnets can be indicative of the spin of the samples, particularly if magnetization data are not normalized by the saturation magnetization. Normalization makes M/M_s vs H curves tend to unity regardless of the spin value; it also makes the curves go rather close to each other. Then, experimental points can appear over magnetization curves corresponding to spin values which do not relate to the data because the paramagnetic behavior of the sample deviates from the ideal model. This has occasionally led to erroneous interpretations in the magnetism of molecular compounds.

The data can be easily fit to more adequate magnetization curves. For values of $T \gg \theta$, say 5θ or more, it may be enough to introduce an effective temperature, given by $T_{\text{eff}} = T - \theta$, in the argument of the Brillouin function. Although the fitted value for θ possesses only a rather qualitative character, the formula well describes the data and provides a reliable spin value. A similar approach is often followed to fit magnetization data in diluted magnetic semiconductors.[38]

To fit the data more completely requires consideration of the presence of antiferromagnetic interactions. The simplest way to proceed is to follow a generalization of the Weiss molecular field theory developed a long time ago by Néel.[39] According to this scheme, an obvious antiferromagnetic arrangement for the magnetic molecules in the lattice is to subdivide it into two equivalent interpenetrating sublattices, A and B, in such a way that A molecules have only B molecules as their nearest neighbors and vice versa. In the case of the radical molecules with low magnetic density and weak magnetic interactions, it seems reasonable to neglect the intra-sublattice exchange interaction between A and B nearest neighbor molecules. In these circumstances molecular field theory considers two different molecular fields, $\mathbf{H}_{\text{m}}^{\text{A}}$ and $\mathbf{H}_{\text{m}}^{\text{B}}$, each acting on the A and B sublattices, respectively. $\mathbf{H}_{\text{m}}^{\text{A}}$ ($\mathbf{H}_{\text{m}}^{\text{B}}$) accounts for the interactions of molecules B (A) on each molecule A (B) and is given by

$$\mathbf{H}_{\text{m}}^{\text{A}} = 2\gamma M_{\text{B}} \qquad \mathbf{H}_{\text{m}}^{\text{B}} = 2\gamma M_{\text{A}}$$

where

$$\gamma = \frac{3k\theta}{Ng^2\mu_{\text{B}}^2 S(S+1)}$$

and θ is considered negative.

Upon application of an external field, $\mathbf{H}_{\text{ext}}$, the total fields acting on A and B molecules are

$$\text{H}_{\text{A}} = \mathbf{H}_{\text{ext}} + 2\gamma M_{\text{B}} \qquad \mathbf{H}_{\text{B}} = \mathbf{H}_{\text{ext}} + 2\gamma M_{\text{A}}$$

Then, the magnetization for sublattices A and **B** is given by

$$M_{\text{A}} = \tfrac{1}{2} Ng\mu_{\text{B}} S B_{\text{S}}(x_{\text{B}})$$

$$M_{\text{B}} = \tfrac{1}{2} Ng\mu_{\text{B}} S B_{\text{S}}(x_{\text{A}})$$

where B_{S} is the Brillouin function with arguments

$$x_{\text{A}} = \frac{g\mu_{\text{B}}\mathbf{H}_{\text{ext}}}{kT}S + 2\frac{3\theta}{g(S+1)T}\frac{M_{\text{B}}}{N\mu_{\text{B}}}$$

$$x_{\text{B}} = \frac{g\mu_{\text{B}}\mathbf{H}_{\text{ext}}}{kT}S + 2\frac{3\theta}{g(S+1)T}\frac{M_{\text{A}}}{N\mu_{\text{B}}}$$

Finally, the total magnetic moment is given by

$$M = M_{\text{A}} + M_{\text{B}}$$

The set of equations that yields each sublattice magnetization must be solved simultaneously, as they are coupled by the fact that M_{A} depends on M_{B} and M_{B} on M_{A}. Moreover, magnetization appears in the arguments of the Brillouin functions and on the left-hand side of the equation, which requires some graphical or numerical method to solve M_{A} and M_{B}.

The experimental data depicted in Figure 5 have been fitted to this set of equations following a standard numerical method. The Curie–Weiss parameters from the susceptibility curves have been used as initial values for θ. For each θ value the sublattice magnetizations were calculated following a self-consistent procedure, where the magnetization of a pure paramagnet or that from a previous fitting cycle was used to initiate the procedure. In either case convergency was reached very rapidly after a few cycles. Best agreement with the data was obtained for $\theta = -0.1$, -0.8, and -0.8 for radicals **2**–**4**, respectively, and is shown in Figure 5 as solid lines. In the case of radicals **2** and **3**, the presence of impurities from radicals **3** and **2** was taken into account. The fitted values of θ are found to be somewhat smaller than those determined from the susceptibility curves. Differences can be attributed to a larger uncertainty in the θ values as calculated by extrapolation from susceptibility measurements. The calculated magnetization curves indicate that the ground states of radicals **2**–**4** are doublet ($S = {}^1/_2$), triplet ($S = 1$), and quartet ($S = {}^3/_2$), respectively, in excellent agreement with ESR and susceptibility results. Consequently, the magnetic measurements reported here indicate that the high-spin states are the ground states of the stereoisomers of polyradicals **3** and **4** and, moreover, the energy gaps between those states and nearby low-spin excited states are far higher than 200 cm^{-1} (the energy equivalent of highest experimental temperatures assayed, i.e., kT_{max}/hc).

In conclusion, the results described here indicate that the intramolecular exchange coupling in the stereoisomers of polyradicals **3** and **4** is strongly ferromagnetic. In addition, they also suggest that perturbations due to the presence of electronegative heteroatoms (Cl substituents), the lack of planarity, and changes in symmetry in a molecule are small, and the topological considerations developed for planar and unsubstituted alternate hydrocarbons[2] can also be applied to highly distorted and heteroatom-substituted conjugated alternate systems. This assumption is supported by the results reported for the stereoisomers of biradical **1**[1] and those described for other heteroatom-perturbed conjugated alternate systems.[6,9,40] The topology seems therefore to be the most important factor in determining the ground-state multiplicity in π-conjugated alternate systems.

Experimental Section

General Methods. ESR spectra were obtained on a Varian E-Line Century Series X-Band ESR spectrometer equipped with a field-frequency lock, a variable-temperature accessory, and a data acquisition system. g values were determined using a T_{104} dual sample cavity with DPPH as standard. The reported ESR spectra were obtained at microwave frequencies in the vicinity of 9.31 GHz with the 100-kHz field modulation detection unit. All precautions were taken to avoid undesirable spectral line broadenings, such as those arising from microwave power saturation and magnetic field overmodulation. Sample solutions

---

(38) Gaj, J. A.; Planel, R.; Fishman, G. *Solid State Commun.* **1979**, *29*, 435.

(39) Néel, L. *Ann. Phys.* (*Paris*) **1936**, *5*, 232. For a description of molecular field theory, see for example: Morrish, A. H. *The Physical Principles of Magnetism*; John Wiley & Sons: New York, 1965. Smart, J. S. *Effective Field Theories of Magnetism*; W. B. Saunders Co.: London, 1966. Herpine, A. *Théorie du Magnetisme*; Presses Universitaires de France: Paris, 1968.

(40) Wasserman, E.; Murray, R. W.; Yager, W. A.; Trozzolo, A. M.; Smolinsky, G. *J. Am. Chem. Soc.* **1967**, *89*, 5076. Seeger, D. E.; Lathi, P. M.; Rossi, A. R.; Berson, J. A. *J. Am. Chem. Soc.* **1986**, *108*, 1251. Tukada, H.; Mutai, K.; Iwamura, H. *J. Chem. Soc., Chem. Commun.* **1987**, 1159. Veciana, J.; Rovira, C.; Armet, O.; Domingo, V. M.; Crespo, M. I.; Palacio, F. *Mol. Cryst. Liq. Cryst.* **1989**, *176*, 77.

were degassed by the freeze–thaw cycle method with the use of an oil pump and were sealed under prepurified dry argon atmosphere. Magnetic susceptibility data were measured, using the Faraday technique, from 80 to 300 K with a Varian 4-in. magnet with constant-force caps and a Cahn RG electrobalance. The measurements were made on samples (ca. 0.01–0.03 g) of monoradical **2** and pure C_2-**4** and also on stereoisomeric mixtures of polyradicals **3** and **4**. The observed magnetic susceptibilities were fitted to the Curie–Weiss law by a least-squares method. Effective magnetic moments were calculated, as usual, from the Curie constant,[41] and θ values were determined by extrapolation of $1/\chi$ up to $T = 0$ K. Susceptibility measurements (ac) were carried out in a computer-controlled susceptometer.[42] The measurements were performed in the temperature range 4.2–25 K and at zero external field; the amplitude of the alternating magnetic field was 1 Oe and the frequency 122 Hz. Magnetization measurements on samples of radicals **2**–**4** (ca. 0.04–0.08 g) were made at 4.2 K, using the same ac susceptometer, by integrating the voltage induced in the secondary coils when the samples were moved in the presence of an external field.

^{1}H NMR spectra were taken on a Bruker WP 80 SY instrument. UV–vis and IR spectra were measured on Perkin-Elmer Lambda Array 3840 and Perkin-Elmer 682 spectrometers, respectively. Cyclic voltammetry was carried out on a PAR 174 A voltammograph using CH_2Cl_2 solutions of radicals **2**–**4** (3×10^{-4} M). Voltammograms were performed at 293 K under argon using a sweep rate of 50 mV s^{-1}. Analytical HPLC was performed on an octadecylsilane (ODS) column (0.46 × 15 cm) with a flow rate of 1.0 mL min^{-1} CH_3CN/THF (70:30) on a Perkin-Elmer Series 3DLC equipped with a Sigma 15 data station and a LC-75 spectrophotometer detector operating at 383 nm. Semipreparative HPLC was performed on an ODS column (1.0 × 25 cm) with a flow rate of 5 mL min^{-1} CH_3CN/THF (60:40) using the same equipment. HPLC columns were thermostated with a homemade jacket using a Hetofrig ultrathermostat with external circulation. Preparative chromatography under flash conditions employed 230–400 mesh silica (SDS, silica gel 60). Melting points were obtained with a Köfler microscope and are uncorrected. Microanalyses were performed at the Microanalysis Service of the Centre d'Investigació i Desenvolupament, CSIC.

THF and toluene were distilled from benzophenone ketyl under argon immediately before use. Reagents and solvents were obtained commercially and used without further purification unless otherwise noted. The handling of radicals in solution was performed under red light or in the dark.

Preparation of α,α,α′,α′,α″,α″,2,4,6-Nonachloromesitylene (6). A mixture of 1,3,5-trichlorobenzene (1.0 g, 5.5 mmol), $CHCl_3$ (20 mL), and powdered anhydrous $AlCl_3$ (0.75 g, 5.6 mmol) was heated at 100 °C for 18 h in a glass pressure vessel and then poured into cracked ice/hydrochloric acid. The organic layer was separated, washed with aqueous $NaHCO_3$ and with water, dried, and concentrated under reduced pressure. Flash chromatography (hexane) of the residue afforded pure **6** (1.52 g, 64%): mp 183–185 °C (lit.[43] mp 187–189 °C); ^{1}H NMR (CCl_4) δ 7.75 (br s). Anal. Calcd for $C_9H_3Cl_9$: C, 25.14; H, 0.70; Cl, 74.20. Found: C, 25.17; H, 0.55; Cl, 74.30.

2,4,6-Trichloro-α,α,α′,α′,α″,α″-hexakis(pentachlorophenyl)mesitylene (7). A mixture of **6** (1.6 g, 3.71 mmol), pentachlorobenzene (13.8 g, 55.36 mmol), and aluminum trichloride (1.6 g, 11.9 mmol) was heated at 140 °C for 18 h in a glass pressure vessel. The mixture was poured into ice/hydrochloric acid and extracted with chloroform. The organic extract was washed with aqueous $NaHCO_3$ and with water, dried, and evaporated. Flash chromatography of the residue (silica gel, hexane) afforded 4.2 g of **7** as a white solid (66%): mp > 305 °C; IR (KBr) 2925, 1530, 1360, 1335, 1310, 1290, 805 cm^{-1}; ^{1}H NMR ($CDCl_3$) δ 6.6–7.5 (m). Anal. Calcd for $C_{45}H_3Cl_{33}$: C, 31.54; H, 0.18; Cl, 68.28. Found: C, 31.44; H, 0.31; Cl, 68.28.

2,4,6-Trichloro-α,α,α′,α′,α″,α″-hexakis(pentachlorophenyl)mesitylene Monoradical (2). Tetrabutylammonium hydroxide (40% in water) (0.066 mmol) was added to a solution of **7** (0.100 g, 0.058 mmol) in tetrahydrofuran (THF) (10 mL), and the resulting mixture was stirred at room temperature (3 h). Then *p*-chloranil (0.018 g, 0.075 mmol) was added and the stirring continued (2 h). Elimination of the solvent gave a residue which was passed through silica gel (CCl_4) to give quantitatively 0.98 g of **2** as a bright red microcrystalline powder. HPLC revealed that the sample contained a small fraction (6%) of diradical **3**. **2**: mp >310 °C; IR (KBr) 2920, 1515, 1370, 1360, 1335, 1310, 1258, 1115, 805 cm^{-1}; UV–vis ($CHCl_3$) 280 (sh) 387, 517, 567 (ϵ 10 720, 53 703, 1348, 1318); ESR (toluene) g 2.0024 ± 0.0003, ^{13}C-α = 3.13 mT, ^{13}C-arom = 1.24 mT; magnetic susceptibility (80–300 K) μ_{eff}, 1.79 μ_B. Anal. Calcd for $C_{45}H_2Cl_{33}$: C, 31.56; H, 0.12; Cl, 68.32. Found: C, 31.61; H, 0.20; Cl, 68.15.

2,4,6-Trichloro-α,α,α′,α′,α″,α″-hexakis(pentachlorophenyl)mesitylene Diradical (3). A great excess of tetrabutylammonium hydroxide (40% in water) (3.3 mmol) was added, under argon and in the dark, to a solution of **7** (0.193 g, 0.11 mmol) in THF (20 mL), and the reaction mixture was stirred at room temperature (5 days). Then *p*-chloranil (0.89 g, 3.63 mmol) was added and the stirring was continued (2-h). Elimination of the solvent afforded a residue which was passed through silica gel (CCl_4) to give 0.152 g (79%) of **3** (mixture of several isomers, as ascertained by HPLC from the presence of several unresolved peaks) as a wine red solid: mp >310 °C; IR (KBr) 1510, 1355, 1335, 1310, 1258, 1110, 815, 810 cm^{-1}; UV–vis ($CHCl_3$) 286 (sh), 388, 514, 563 (ϵ 11 967, 61 659, 2830, 2818); magnetic susceptibility (80–300 K) μ_{eff}, 2.87 μ_B. Anal. Calcd for $C_{45}HCl_{33}$: C, 31.58; H, 0.06; Cl, 68.36. Found: C, 31.42; H, 0.17; Cl, 68.21.

2,4,6-Trichloro-α,α,α′,α′,α″,α″-hexakis(pentachlorophenyl)mesitylene Triradical (4). A great excess of tetrabutylammonium hydroxide (40% in water) (18 mmol) was added, under argon and in the dark, to a solution of **7** (0.7 g, 0.41 mmol) in THF (50 mL), and the reaction mixture was stirred at room temperature (35 days). Then *p*-chloranil (5.6 g, 20.2 mmol) was added and the stirring was continued (2-h). Elimination of the solvent afforded a residue which was passed through silica gel (CCl_4) to give 0.273 g (39%) of **4** (C_2 and D_3 isomers in a molar ratio of 82:18, as ascertained by HPLC) as a dark red solid: mp >310 °C; IR (KBr) 1510, 1340, 1325, 1310, 1260, 822, 800 cm^{-1}; UV–vis ($CHCl_3$) 292 (sh), 388, 508, 558 (ϵ 18 132, 91 200, 4570, 4365); magnetic susceptibility (80–300 K) μ_{eff}, 3.86 μ_B. Anal. Calcd for $C_{45}Cl_{33}$: C, 31.58; Cl, 68.42. Found: C, 31.48; Cl, 68.49. Recrystallization from benzene gave pure C_2 isomer (HPLC) as a dark red crystalline powder: mp >310 °C; magnetic susceptibility (80–300 K) μ_{eff}, 3.89 μ_B. Anal. Calcd for $C_{45}Cl_{33}$: C, 31.58; Cl, 68.42. Found: C, 31.64; Cl, 68.39.

Acknowledgment. This work was supported by C.I.C. y T. (Grant MAT91-0553). The authors thank Prof. J. Claret (Universitat de Barcelona) for CV measurements and for his kind suggestions and also Mrs. A. Diez for operating the ESR spectrometer and the Faraday magnetometer. N.V. thanks C.I.R.I.T. for a grant.

Registry No. 2, 144811-64-3; **3**, 144811-65-4; **4**, 127335-78-8; **5**, 108-70-3; **6**, 40860-87-5; **7**, 144811-66-5; $CHCl_3$, 67-66-3; C_6HCl_5, 608-93-5; *n*-$Bu_4N^+OH^-$, 2052-49-5; *p*-chloranil, 118-75-2.

---

(41) Carlin, R. L. *Magnetochemistry*; Springer: New York, 1986.

(42) Rillo, C.; Lera, F.; Badía, A.; Angurel, L. A.; Bartolomé, J.; Palacio, F.; Navarro, R.; Van Duyneveldt, A. J. In *Magnetic Susceptibility of Superconductors and Other Spin Systems*; Hein, R. A., Francavilla, T. L., Liedenberg, D. H., Eds.; Plenum Press: London, in press.

(43) Peeling, J.; Goodwin, B. W.; Schafer, T.; Rowbotham, J. B. *Can. J. Chem.* **1973**, *51*, 2110.